SYNTHESIS AND CHARECTERIATION OF MANGANESE OXIDE NANAPARTICLES

Submitted in partial fulfillment of the requirements for the award of Master of Science degree in Physics

By

MAADHAVAN (40590018)

DEPARTMENT OF PHYSICS

SCHOOL OF SCIENCE AND HUMANITIES

SATHYABAMA

INSTITUTE OF SCIENCE AND TECHNOLOGY

(DEEMED TO BE UNIVERSITY)

Accredited with Grade"A" by NAAC

JEPPIAAR NAGAR, RAJIV GANDHI SALAI, CHENNAI - 600119

MAY–2022

SATHYABAMA
INSTITUTE OF SCIENCE AND TECHNOLOGY
(DEEMED TO BE UNIVERSITY)
Accredited "A" Grade by NAAC | 12B Status by UGC | Approved by AICTE
www.sathyabama.ac.in

DEPARTMENTOF PHYSICS

BONAFIDE CERTIFICATE

This is to certify that this Project Report is the bonafide work of **M.MAADHAVAN (Reg.No.40590018)** who carried out the project entitled "**SYNTHESIS AND CHARECTERIATION OF MANGANESE OXIDE NANAPARTICLES**" under my supervision from **NOVEMBER 2021 to MARCH 2022**

Dr. Anita Lett

Head of the Department

Dr.S.RAVICHANDRAN

Submitted for Viva voce Examination held on_____

Internal Examiner **External Examiner**

DECLARATION

I **M.MAADHAVAN (Reg.No.40590018)** hereby declare that the project report entitle "**SYNTHESIS AND CHARECTERIATION OF MANGANESE OXIDE NANAPARTICLES"** done under the guidance of **Dr. Anita Lett** is submitted in partial fulfillment of the requirements for the award of Master of Science degree in Physics.

DATE:

PLACE: **SIGNATURE OF THE CANDIDATE**

ACKNOWLEDGEMENT

I am pleased to acknowledge my sincere thanks to the Board of Management of **SATHYABAMA** for their kind encouragement in doing this project and for completing it successfully. I am grateful to them.

I convey my thanks to **Dr. S. Ravichandran**, Head of the Department, and Department of Physics for providing me necessary support and details at the right time during the progressive reviews.

I am thankful to My Parents and Family members for their constant support in completion of the project.

I would like to express my sincere and deep sense of gratitude to my Project Guide **Dr. Anita Lett** for their valuable guidance, suggestions and constant encouragement that paved way for the successful completion of my project work.

I wish to express my thanks to all Teaching and Non-teaching staff members of the Department of Physics who were helpful in many was for the completion of the project.

---------- Finally, without the help of my friends, who supplied intriguing discussion, I could not have been able to accomplish this project.

(M.MAADHAVAN)

ABSTRACT

In this work, a simple, efficient and procedure for the green synthesis of manganese oxide nanoparticles (Mn_2O_3 NPs) by hydrothermal synthesis is described. Fourier-transform infrared spectra revealed the the formation of Mn_2O_3 NPs. The ultraviolet–visible absorption spectra of the synthesised Mn_2O_3 NPs exhibited absorption peaks at 410 nm, which were attributed to the band gap of the Mn_2O_3 NPs. Crystal phase identification of the Mn_2O_3 NPs was characterised by X-ray diffraction analysis and the formation of crystalline Mn_2O_3 NPs has been confirmed. Also, the X-ray diffraction pattern displayed that the average size of Mn_2O_3 NPs was about 80 nm. Furthermore, scanning electron microscopy analysis showed that the synthesised Mn_2O_3 NPs have a spherical shape. Mn_2O_3 NPs have photocatalytic activities for the dye degradation in the visible light region. The photocatalytic activities for the dye degradation of Mn_2O_3 NPs were evaluated using Acid Orange as an organic contaminant.

TABLE OF CONTENT

S. NO.	LIST OF CONTENT	PAGE NO
1.	**CHAPTER 1: INTRODUCTION**	**1-3**
2.	**CHAPTER 2: LITERATURE SURVEY**	**4-7**
3.	**CHAPTER 3: AIM AND SCOPE**	**8**
3	**3.1 Aim of the investigation**	**8**
4.	**CHAPTER 4: MATERIALS AND METHODS**	**9-14**
4.1	**SYNTHESIS OF MN_3O_4 NANOSTRUCTURE**	**9**
4.2	**X-ray diffraction**	**10-11**
4.2.1	**Application**	**11**

4.3	**Fourier transform infrared spectroscopy**	**12-13**
4.4	***Scanning Electron Microscope***	**13-14**
4.4.1	**Application**	**14**
4.5	**Photo-catalytic measurement**	**14-15**
5	**CHAPTER 5: RESULT AND DISCUSSION**	**15-20**
5.1	***Structural analysis***	**15-16**
5.2	**FTIR Spectroscopy**	**16-17**
5.3	**Scanning Electron Microscope (SEM)**	**17-18**
5.4	**Optical studies - UV-Visible Spectroscopy**	**18-19**
5.5	***UV-Visible Spectra of Manganese oxide nanoparticles***	**19-20**

6	**CHAPTER 6: SUMMARY AND CONCLUSION**	**20**
	REFERENCE	**21-26**

LIST OF ABBREVIATIONS

- SEM –SCANNING ELECTRON MICROSCOPE
- XRD –X-RAY DIFFRACTION
- EDX – ENERGY DISPERSIVE X-RAY
- $TiSi_2$ - TITANIUM DISILICIDE
- CVD – CHEMICAL VAPOUR DEPOSITION
- PVD – PHYSICAL VAPOUR DEPOSITION
- AFM –ATOMIC FORCE MICROSCOPE

LIST OF FIGURES

FIG NO	TITLE	PAGE NO
1.1	*Schematic representation for synthesis of Mn_2O_3 NPs*	9
4.2	*X-ray Diffraction*	10
4.3	*Fourier transform infrared spectroscopy*	12
4.4	*Scanning Electron Microscope*	13
5.1	Powder XRD patterns of Mn_3O_4 NPs.	16
5.2	FT-IR Spectrum of Mn_2O_3 nanoparticles	16
5.3	*SEM images of as prepared* Mn_3O_4 *nanoparticles*	17
5.4	EDAX Spectrum of Mn3O4 nanoparticles	18
5.5	*UV-Visible Spectra of Manganese oxide nanoparticles*	19

LIST OF TABLE

CHAPTER 1

INTRODUCTION

Nanomaterials, having a length scale less than 100 nm, have received increasing interest owing not only to their fundamental scientific significance but also to the potential applications that derive from their fascinating electrical, magnetic, and catalytic properties [1]. Compared to bulk active electrode materials, the corresponding nanomaterials possess more excellent electrochemical activity, such as higher capacities, larger surface areas, and lower current densities, thereby, nonmaterial have wildly potential application in electro- chemistry field. Manganese oxides, including MnO, MnO_2, and Mn_3O_4, are intriguing composites and have been used in wastewater treatment, catalysis, sensors, supercapacitors, and alkaline and rechargeable batteries [2–6]. Particularly, MnO and MnO_2 nanomaterials have attracted great interest as anode materials in lithium-ion batteries (LIBs) for their high theoretical capacity, low cost, environmental benignity, and special properties [7–9].

Now a day's nanotechnology attained a great interest due to the recent developments in the science and engineering fields, nanotechnology can be deliberated as technology of [10]. Nanotechnology developed numerous types of materials at nanoscale level. In current years, quick advancement in the nanotechnology field has facilitated the development of engineered nanoparticles of different kinds, dimensions, and morphologies [11]. Nanoparticles are extensive kinds of materials that embrace particulate materials, which have one dimension below 100 nm at least [12]. They can maintain physico-chemical properties such as high surface area, conductance, homogeneity, structural stability or distinct optical properties etc., that make them required in materials science and various application fields [13]. These nanoparticles have made a tremendous impact in the various applications such as catalysis, pharmaceutics, optics, food technology, cosmetics, water treatment, electrochemistry, energy, biomedicine, biosensor cancer treatment, healthcare and drug delivery [14], The nanoparticles properties in the medicinal arena were improved greater associated to their bulk counterparts. In this nanomaterial's metal and metal oxide nanoparticles display distinct physical

and chemical properties, particularly metal oxide nanomaterial's are enormously stimulating in the field of semiconducting constituents and endorse an ideal prospect for the progress of biological activities [15-17]. In these nanomaterials, trimangnese tetraoxide nanoparticles (Mn2O3) is one of the significant nanoparticles comprise of various crystal structures constructed from octahedral MnO_6 were, manganese dioxide (MnO_2), dimanganese trioxide (Mn_3O_4) [18-20]. There are a diversity of approaches to develop metal/metal oxide NPs, for instance precipitation, hydrothermal, microemulsion, sol–gel, and sonochemical technique, which usually provide adequate products for various applications [21-23]. Manganese oxides is a mixed oxide material are appropriate for wide range applications such as catalysis, electrochemical, medicinal due to their low cost, eco-friendly nature, existence of manganese in various states and their natural abundance [24-25].

The numerous manganese oxidation states consequences in the development of manganese dioxide, dimanganese trioxide, trimanganese tetraoxide. In these, Mn2O3nanoparticles have encouraged abundant attention owing to their distinctive structural and electronic features with exclusive ion exchange, catalysis, molecular adsorption, magnetic and electrochemical properties. Manganese is deliberated a vital constituent in metabolism has been well controlled by biological systems and Mn_3O_4 NPs display greater biological properties and low toxicity [26-28]. Accordingly, Mn2O3 NPs have been competently examined as prospective antibacterial systems because of their synergistic performance. The ions 'Mn2+' generates harmless free radicals, which performance a vital part in clinical sicknesses like Alzheimer's, cardiac, diabetes, numerous diseases etc., including cancer, and moreover, nanomedicine is supposed to be a favorable investigation route in the tumors treatment (Khan et al., 2016). In the current scenario, the major complication in cancer treatment is the partial existence of particular anticancer drugs or nanomedicines along with a lesser amount of competent delivery systems and majority of the currently existing anticancer drugs having poor solubility in aqueous solutions. Consequently, major efforts have been carried out to generate novel anticancer drugs with superior aqueous solubility and effective in cancer treatment. Among them, metal oxide nanoparticles have synergistic and superior physicochemical properties made huge

attention in cancer treatment [29-30]. In the current work, we demonstrate a precipitation method for the synthesis Mn2O3 nanoparticles using manganese nitrate as a precursor material by utilization of a precipitation method (Scheme 1). As-synthesized Mn2O3nanoparticles characterized by several microscopic, spectroscopic and thermal techniques such as SEM, EDX, UV–Vis, XRD, FT-IR. The biological properties of the as-prepared Mn_3O_4 NPs were investigated against various fungal and bacterial strains comprising S. aureus, B. subtilis, E. coli, P. aeruginosa, C. albicans and A. flavus. The growth of S. aureus inhibited with a MIC of 40 lg/ml and C. albicans with a MIC of 15 lg/ml using Mn2O3 NPs.

CHAPTER 2

LITERATURE SURVEY

Marugán et al [31] in this work executes a complete thermodynamic study of the first step of the Mn_2O_3/MnO thermochemical cycle for solar hydrogen production has been performed. The thermal reduction of Mn_2O_3 takes place through a sequential mechanism of two reaction steps. Finally, this work demonstrates that the first step of the manganese oxide thermochemical cycle for hydrogen production can be carried out with total conversion at temperatures compatible with solar energy concentration devices. The range of required temperatures is lower than those commonly reported in literature for the manganese oxide cycle obtained from theoretical and thermodynamic studies.

Aparna Iyer et al [32] aim was to split water into hydrogen and oxygen. However, water oxidation occurs readily in plants, catalyzed by the Mn4O4Ca manganese cluster. In addition to this, manganese minerals are ubiquitous in nature displaying layered and tunnel structures. In this study, mixed valent porous amorphous manganese oxides (AMO), along with cryptomelane type tunnel manganese oxides (OMS-2) and layered birnessite (OL-1) have been used as water oxidation catalysts. Significantly higher turnovers were obtained with AMO (290 mmol O2/mol Mn) compared to tunnel structure OMS-2 (110 mmol O2/mol Mn) and layered structure OL-1 (27 mmol O2/mol Mn) in water oxidation tests with Ce4+. Oxygen evolution was also confirmed under photochemical conditions using Ru(bpy)3 2+ as a photosensitizer and persulfate as a sacrificial agent.

S. Ardizzone et. al [33] prepared α-Mn_2O_3 powders by calcining $Mn(NO_3)_2 \cdot 6H_2O$ at 600°C by a two step procedure. The electrification behaviour of the oxide at the solution boundary was characterised by the determination of charge and capacitance vs. pH curves. The specific pattern observed at high KNO_3 concentrations is interpreted by invoking the occurrence of a solution-supported disproportionation reaction of Mn(III).

Chung-Hao Kuo et al [34] Inspired by the natural oxygen evolution reaction of Photosystem II, the earth-abundant and inexpensive manganese oxides (Mn2O3) have been recognized for their great potential as highly efficient and robust materials for water oxidation reaction (WORs). To date, most of the heterogeneous, synthesized MnO_x catalysts still exhibit lower activities for WORs, in comparison to RuO_2 and IrO_2. Herein, they reported a single-step and scalable synthesis method for mesoporous MnO_x materials that is developed through a soft-templated method.

3Katlego Makgopa et al [35] examinated the pseudocapacitive performance of nitrogen-doped and undoped reduced graphene oxide/tetragonal hausmannite nanohybrids (N-rGO/Mn3O4 and rGO/Mn2O3) synthesized using a one-pot hydrothermal method is reported. The nanohybrid electrode materials displayed exceptional electrochemical performance relative to their respective individual precursors (i.e., reduced graphene oxide (rGO), nitrogen-doped reduced graphene oxide (NrGO), and tetragonal hausmannite (Mn2O3)) for symmetric pseudocapacitors

Ren Z et al [36],In this study, manganese oxide nanoparticles were synthesized through a simple hydrothermal method and applied for the removal of thallium(I). The adsorbent was composed of numerous needle-like nanorods and had an average volume diameter of 230 nm after heat-drying procedure. The crystal form of adsorbent was determined as α-MnO2. The adsorbent exhibited a much faster adsorption rate than most of previously reported adsorbent, achieving over 66.4% of equilibrium adsorption capacity in the first 10 min. The adsorption process was found to be highly affected by solution pH and higher than 100 mg/g of adsorption capacity could be obtained in a wide pH range of 6.0–10.0.

Hendrik Antoni et al [37], have developed nonprecious catalysts for water splitting into hydrogen and oxygen is one of the major challenges to meet future sustainable fuel demand. Herein, thin layers of manganese oxide nanosheets supported on nitrogen-functionalized carbon nanotubes (NCNTs) were formed by the treatment of NCNTs dispersed in aqueous solutions of KMnO4 or CsMnO2

under reflux or under hydrothermal (HT) conditions and used as electrocatalysts for the oxygen evolution reaction (OER) in alkaline media and significantly more efficient purification sequence involving partial oxidation of the as-received CNTs in HNO3 vapor followed by washing in 1.5 M nitric acid was chosen for the subsequent investigations.

Ho, P.H et al [38] in this study the Properties of porous manganese oxide adsorbents for adsorptive removal of tert-butylmercaptan (TBM) from CH4 fuel gas were investigated at ambient temperature and atmospheric pressure. The adsorbents were prepared by oxidation reactions of Mn2+ with KMnO4 and via the sol-gel method by reduction of KMnO4 using fumaric acid as the reducing agent. The effects of preparation method, precursor, temperature, and time for the structure and desulfurization properties of the resulting adsorbents were studied.

Phuoc Hoang Ho et al [39] studies the properties and characteristics of cryptomelane manganese oxide octahedral molecular sieve (OMS-2)-based adsorbents for the adsorptive desulfurization of dimethyl sulfide (DMS), tertbutylmercaptan (TBM), and tetrahydrothiophene (THT) were investigated at ambient temperature and atmospheric pressure. OMS-2 adsorbents exhibited above 90% adsorption selectivity for TBM in a ternary mixture of DMS, TBM, and THT in a methane fuel stream, which is unique and unprecedented for zeolite-, metal oxide- , and activated carbonbased adsorbents

Navin Kumar Chandra et al [39] parpared nano-size crystals of Mn2O3 and by a simple precipitation process using dilute aqueous solutions of manganese sulphate and ammonia in the presence of sodium lauryl sulphate — a surface active agent. X-ray diffraction spectrometry has been used to identify the phases and to calculate the size of the nano-size crystals using the Scherrer method. The morphology of the crystals has been studied by TEM/ HRTEM and Edax has been used to estimate their elemental constituents. The sonication of the prepared nano-size material in acetone leads to the conversion of MnOOH to nano-sized Mn2O3

Lin, C. K et al [40] in this study, manganese oxide electrodes with promising pseudo-capacitive behavior were prepared by sol–gel process using manganese acetate as the precursor. Effects of postheat treatment on material characteristics and electrochemical properties were investigated

CHAPTER-3

3.1 Aim of the investigation

Manganese oxides is a mixed oxide material are appropriate for wide range applications such as catalysis, electrochemical, medicinal due to their low cost, eco-friendly nature, existence of manganese in various states and their natural abundance. Thus keeping these factors in mind, the aim of this investigation undertaken are

- Synthesis of Manganese – oxide nanoparticles
- Characterization of the material synthesized:
  - X-ray diffraction (XRD)
  - Fourier transform infrared spectroscopy (FTIR)
  - Scanning electron microscopy (SEM)
  - Energy dispersive X-ray spectroscopy (EDAX)
  - Antibacterial studies

CHAPTER - 4

MATERIALS AND METHODS

4.1 SYNTHESIS OF MN_3O_4 NANOSTRUCTURE

For the formation of Mn_3O_4 NPs, 1.0 g Polyvinyl alcohol (PVA) and 2 mmol manganese acetate were dissolved in 100 mL distilled water with magnetic stirring at 90 °C for 30 min. From this, the solution mixture was transferred to a Teflon-lined autoclave. The autoclave was sealed and subjected to a temperature of 120 °C for 12 h and then cooled to room temperature. On cooling, the precipitate gets formed was filtered, washed with distilled water and ethanol several times (to remove the soluble nitrates). Finally, dried in an oven at 80 °C for 12h. Finally, the dried precipitates were annealed at 1000 °C under air for 3 h to obtain the Mn_2O_3 NPs which have been stored until further use. The schematic representation of Mn_2O_3 NPs formation by the hydrothermal synthesis route is provided in Figure 1.

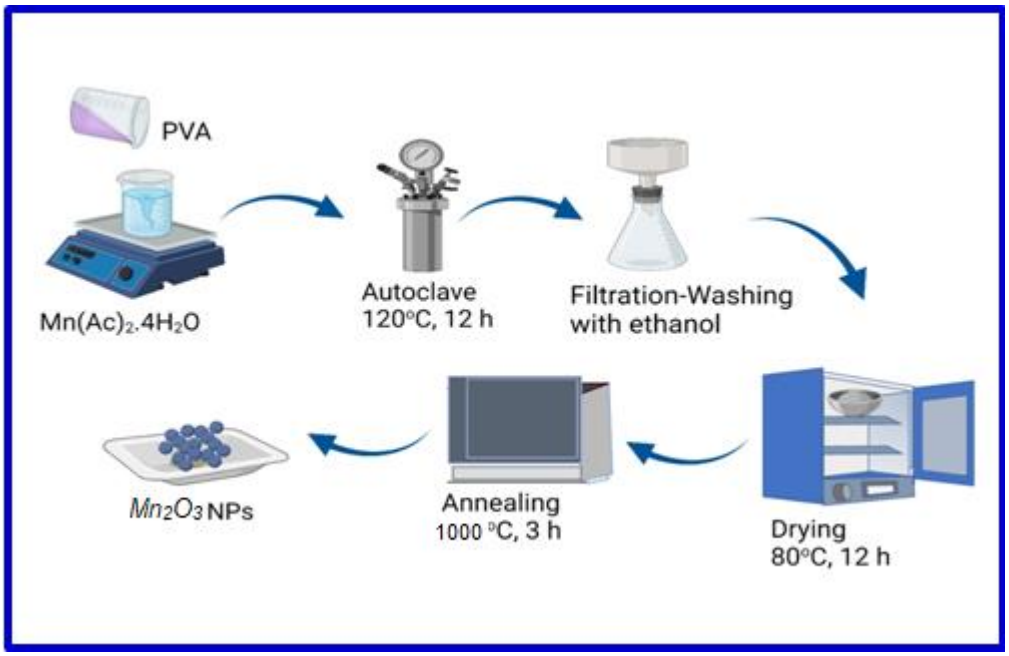

Fig. 1 Schematic representation for synthesis of Mn_2O_3 NPs

4.2 X-ray diffraction

This is used to identify the crystallinity of the material and it gives the unit cell dimensions information. It was founded in 1895 by Wilhelm Rontgen later it was developed by Max von Laue in 1912. It is mostly used in research fields,it can be obtained by orientation at different temperatures but it doesn't give information about its chemical nature. It is a powerful non-destructive device.

Fig 4.2 X-ray Diffraction

x-rays are waves of electromagnetic radiation. When we place our materials they scatter incident x-rays through interaction with the atom's electrons. This is known as elastic scattering. The electrons strike heavy target materials that are cathode rays. The regular array of scatterers gives a regular array of spherical waves. Thus it has some condition that successive lines of the grating will be equal to the wavelength of light. In most of the directions, the destructive interference cancels each other but they add constructively in a specific direction by Bragg's law. The wavelength of light should be Armstrong range and the most important condition is that spacing between atoms should be equal to the wavelength of x-ray. It consists of a glass tube that is to evaluate for high temperature. There are two parts cathode

which contains filament and anode for x-ray targeting. Bragg's law states:-2dsinθ = nλ, where d is the spacing between diffracting plane, θ is the incident angle, n is an integer and λ is the wavelength. Continuously x-ray diffraction patterns show electromagnetic waves spotting on a regular array of scatterers(55).

4.2.1 APPLICATIONS

To find the crystalline or amorphous materials whether it is minerals or an inorganic compound and it is a non-destructive method. It requires only a minimal sample for analysis. To identify the orientation and to determine structural properties like lattice parameters, phase composition, strain and epitaxy. To measure the thickness of thin films and multilayers and to determine the atomic arrangement.

4.3 Fourier transform infrared spectroscopy

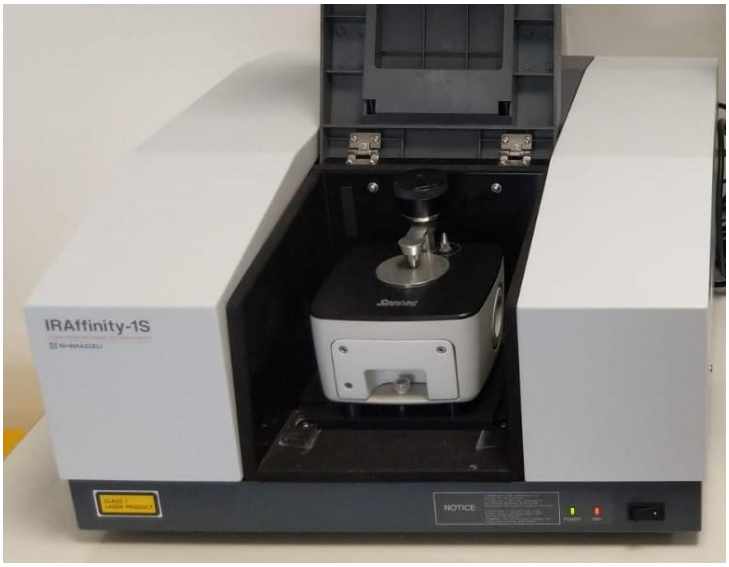

Fig 4.3 *Fourier transform infrared spectroscopy*

Fourier transform infrared spectroscopy studies the interaction of infrared light with matter. Analysis of infrared spectrum can give both quantitative and qualitative analysis i.e. it can tell what type of molecules are present in a sample and at what concentrations. Generally, FTIR is used to identify the functional groups

present in the sample. This technique can obtain spectra from wide number of samples in gas, liquid or solid state and study their structure. The Michelson interferometer is the heart of all modern FTIR spectrometers. It consists of a beam splitter, a fixed mirror, and a moving mirror.

Fourier Transform Spectroscopy is a simple mathematical technique to resolve a complex wave into its frequency components. The conventional IR spectrometers are not of much use for the far IR region, as the sources are weak and the detectors are insensitive. FTIR has made this energy-limited region more accessible. It has also made the mid–infrared (4000-400 cm^{-1}) more useful. In the Fourier Transform Spectrometer, a time domain plot is converted into a frequency domain spectrum. The interference pattern is obtained from a two-beam interferometer, as the path difference between the two beams is altered, then fourier transformed output gives rise to the spectrum. Solid samples are dispersed in KBr or polyethylene pellets depending on the region of interest.

FTIR analysis measures a sample's absorbance of infrared light at various wavelengths to determine the material's molecular composition and structure. However, it is easier to consider transmittance instead of absorbance, so the FTIR graph is transmittance (percentage) vs. wavenumber plot.

4.4 SCANNING ELECTRON MICROSCOPE

Scanning electron microscope(SEM) is the improvement of an electron microscope. It scans a focused stream of electrons over a surface to form an image. It was founded by Stintzing in 1927 later it went through a lot of improvements. Its principle involves the interaction of electrons with the atoms of an object. The image is formed by detected signal and merging beams. It has been built by a single electron gun, with no uses for auxiliary lenses(56)

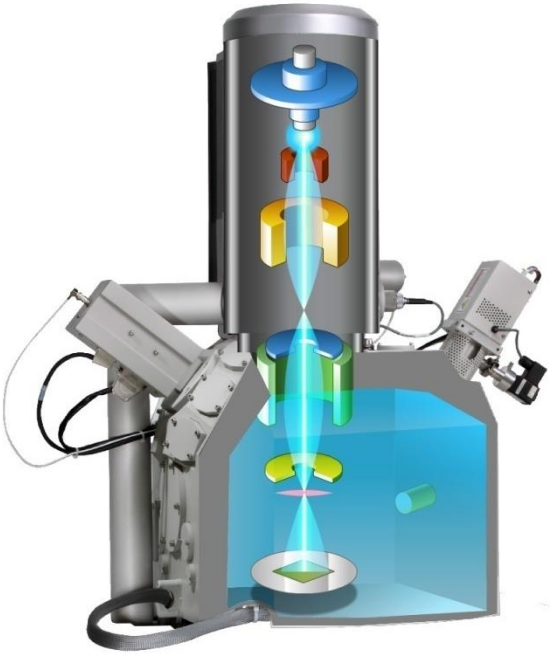

Fig 4.4 Scanning Electron Microscope

When primary electrons strike's the samples it produces the secondary electron, in this secondary electrons contains information about the object and give the 3D images of the samples. The SEM consists of an electron gun that produces a high energy electron beam a voltage is applied for the control of the emission current and the tungsten tip, the magnetic condensing lens is used for condensing the electron beam. The scanning coil is placed between condense lens and sample, the scintillator is present to collect the secondary electrons which convert into an electrical signal. This electrical signal can be fed into CRO through a video amplifier. It can be directly viewed on-screen, to examine large thickness and used in a large depth of focus. When the rays hit on the sample there will be emission of three types of beam outside of the sample that is x-ray, back reflection and secondary electrons.

4.4.1 APPLICATIONS

Used in examining the structure of very large 3D images. The results of the samples get with resolution down to the nanometer scale. Mainly used for the surface that is for topography that how it looks texture, detectable features. Then we can get the details by elemental analysis of how the atoms are arranged. It helps to examine a wide range of materials at high and low magnification without focusing on depth.

4.5 Photo-catalytic measurement

We have examined the photo-catalytic activity of the formed nanopowder using Methylene blue (MB) dye. The 40mg of the sample was used to degrade the 80 ml of MB dye (2.10-5 mol/L) under direct sunlight for 120 mins and the samples were collected in the interval of 15 min. Before starting the experiment, the samples were stirred in room temperature at dark condition for 30 mins. The characteristic absorption band of methylene blue is a single peak at 665 nm in the visible region. The absorption intensity of dyes decreased significantly in the presence of light in comparison with reaction at dark with photocatalyst, which confirms the effective degradation ability of the sample. The variation of the ratio of the concentration (C) after irradiation to the initial concentration (C0) as a function of irradiation time with different photocatalysts is also derived and presented.

The degradation efficiency of MB dye depending on its absorbance (concentration) which can be calculated by the following relation:

$$Efficiency = \frac{(C_0 - C)}{C_0} \times 100\% = \frac{(A_0 - A)}{A_0} \times 100\% \quad (1)$$

Where C0, C, A0, A are concentration and absorbance of MB dye before and after exposing to visible light irradiation, respectively.

CHAPTER-5

RESULT AND DISCUSSION

5.1 Structural analysis

The typical XRD patterns presented in Fig. 5.1 were identified as Mn_3O_4 (JCPDS Card No.00-001-1127) with tetragonal crystal structure (space group 141/amd). Crystallite size of the Mn_3O_4 NPs was calculated from diffraction peaks using the Debye-Scherrer approximation [23]. The crystallite sizes measured from the peaks (112, 103, 211, 004, 220, and 224) were averaged to obtain the crystallite size to be 21 ± 2 nm. Also, as provided in the figure, the diffraction patterns formed are of high sharp, narrow, and are with significant intensity where all these factors support the crystalline nature of the formed Mn_3O_4.

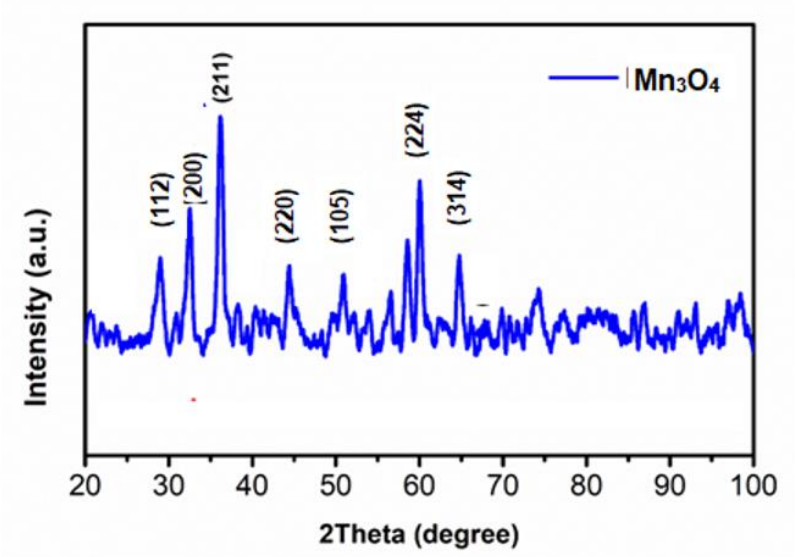

Figure 5.1 Powder XRD patterns of Mn_3O_4 NPs.

5.2 FTIR Spectroscopy:

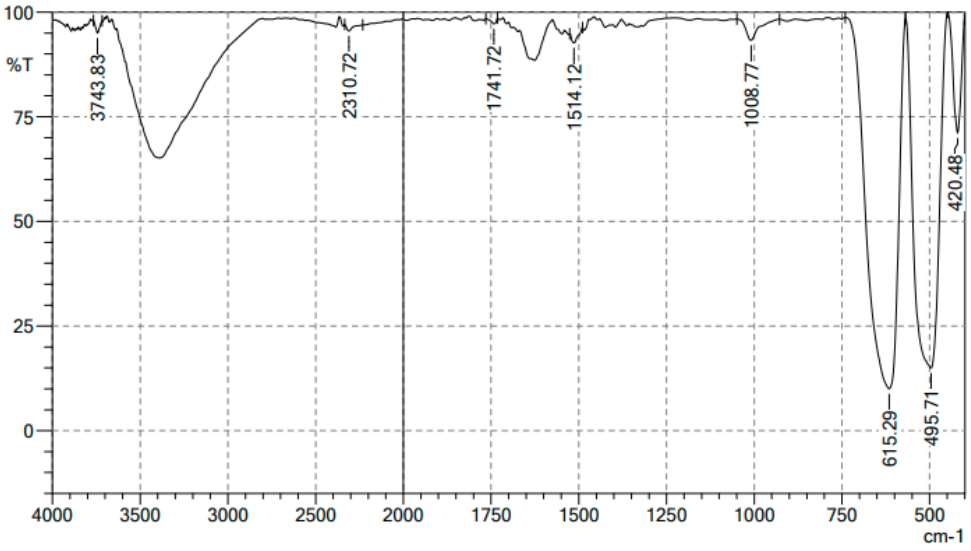

Fig 5.2 FT-IR Spectrum of Mn_2O_3 nanoparticles

Figure 5.2 shows Fourier Transform Infrared (FTIR) Spectrum of the as-prepared Mn_3O_4 products, displaying a notable resemblance to those of Mn_3O_4 obtained in previous studies [32,12]. In the region from 650 to 500 cm^{-1} of the observed spectrum, two absorption peaks were observed at 609 and 503 cm^{-1}, which may be associated with the coupling modes between the Mn-O stretching modes of tetrahedral and octahedral sites. In the region from 500 to 400 cm^{-1}, the absorption peak at 430 cm^{-1} was assigned as the band-stretching mode of the octahedral sites; the displacement of the Mn^{2+} ions in tetrahedral sites was negligible. Therefore, the FTIR spectra further confirm the formation of Mn_3O_4 products.

Furthermore, the characteristic narrow band and broad band situated at 3420 and 1600 cm1 were corresponded to the hydroxy (OH) should be absorbed by the samples or KBr. These FT-IR analysis outcomes are reliable with the evidence achieved from further performed characterization outcomes.

5.3 Scanning Electron Microscope (SEM)

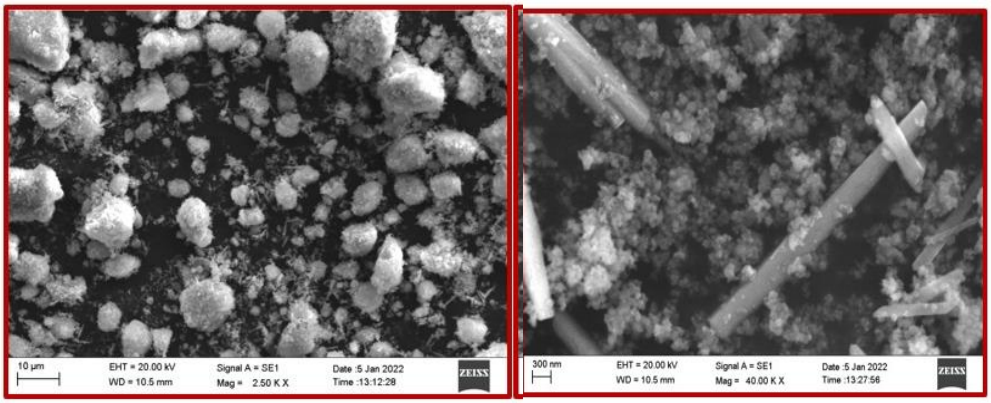

Fig. 5.3. SEM images of as prepared Mn_3O_4 *nanoparticles*

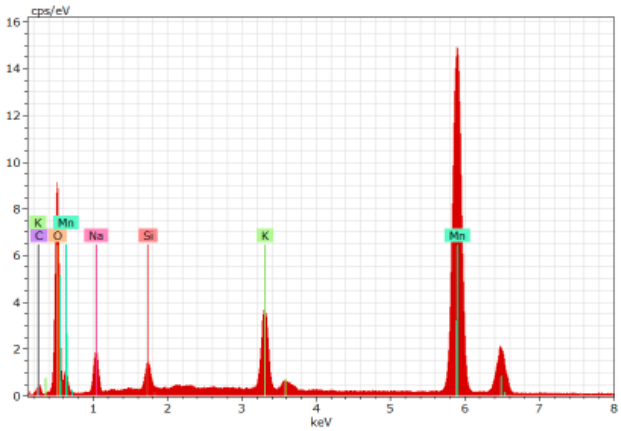

Fig 5.4. EDAX Spectrum of Mn3O4 nanoparticles

The surface morphological studies of nanoparticles have been performed by Scanning Electron Microscope (SEM). The SEM images of Mn2O3 nanoparticles are portrayed in Fig 5.3. It was well documented that the surface morphology has significant impact on the performance of nanostructure materials. The uniform distributions of grains are observed in the micrographs. The particles are nearly spherical in shape has uniform size and found to have an average size of about 50 nm. Fig 5.4 depicts the Energy dispersive X-ray analysis (EDAX) spectrum of Mn2O3 nanoparticles. The presence of Manganese (Mn) and oxygen (O) are confirmed as observed from the EDAX spectrum, some impurities found in the synthesized Mn2O3 nanoparticles were eliminated during annealing process at 1000°C. The chemical composition and product purity of the Mn_3O_4 nanoparticles have been examined by EDAX. The oxygen storage capacity of the prepared sample has been confirmed by observing a peak due to oxygen in EDAX spectrum.

5.4 Optical studies - UV-Visible Spectroscopy

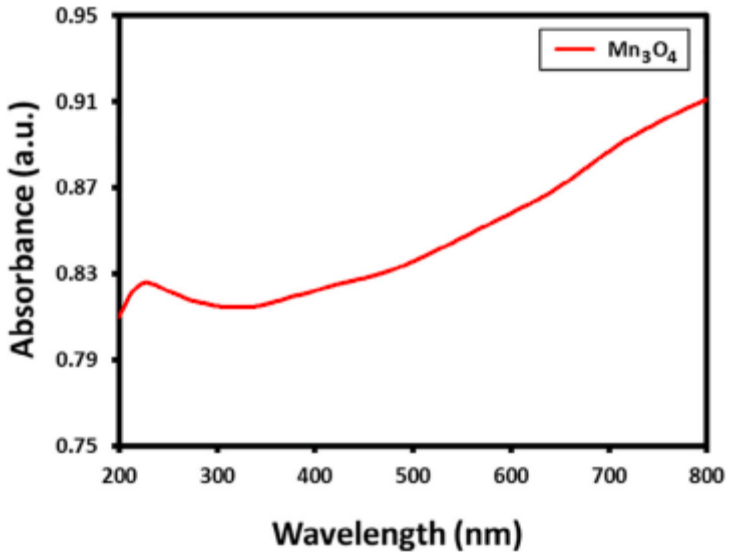

Fig 5.5 UV-Visible Spectra of Manganese oxide nanoparticles

Primarily, the Mn_3O_4 nanoparticle development was examined via UV–Visible analysis, Fig. 15.5. exhibits the UV–Vis spectra of as-prepared Mn_3O_4 nanoparticle using manganese nitrate. The UV–Vis spectra of Mn_3O_4 nanoparticles characteristic peak at ~ 220 nm clearly indicating the Mn_3O_4 nanoparticle formation. [14-15].

Antimicrobial Studies

Zone of Inhibition results of the susceptibility of different microbial stains tested against standard antibiotics

Zone of Inhibition (nm)	Mn_3O_4 NPs	Anti-microbial Gentamycin 50µg/ml	Anti-microbial Fluconazole 50µg/ml
E. coli	10mm	21mm	-
S. aurues	19mm	22mm	-
P. aeruginosa	12mm	21mm	-
B. subtilis	18mm	21mm	-
C. albicans	18mm	-	20mm

Our antimicrobial results were in agreement with Azhir et al., 2015 where E. coli shown to be sensitive and S. aurues showing susceptibility towards Mn3O4 NPs, whereas reports from (Chowdhury et al., 2009) shown E. coli is susceptible. Packirisamy et al., displayed the same results where B. subtilis is susceptible and E. coli and P. aeruginosa also susceptible as anti-microbial activity increased by increasing the concentration (Packirisamy et al., 2019). The Mn_3O_4 NPs inhibited the growth of S. aureus with a minimum inhibitory concentration (MIC) of 40 lg/ml

and C. albicans with a MIC of 15 lg/ml. The results indicate that the asprepared Mn3O4 NPs prepared from manganese nitrate using precipitation approach is a favorable contender for usage pharmaceutical industries and food packaging applications.

CHAPTER-6

SUMMARY AND CONCLUSION

Mn_3O_4 NPs successfully achieved by using precipitation approach. The as-synthesized Mn3O4 nanoparticles are uniformly distributed and well dispersed and tetragonal in shape. The characterization of Mn3O4 nanoparticles was performed by UV–Vis, FT-IR, XRD, SEM, and EDX analysis. The results have exposed the development of tetragonal shape with an average size of 36 nm. The prepared Mn3O4 nanoparticles were assessed for their biological activity. Furthermore, the antibacterial properties, the zone of inhibition, and the minimum inhibitory concentration of Mn3O4 nanoparticles displayed the inhibitory effect against all tested bacteria. Though, the Mn3O4 nanoparticles were found to be selective against S. aureus, & B. subtilis gram positive bacterial strains. Both Gram positive bacteria S. aureus & B. subtilis shown susceptibility towards Mn3O4 nanoparticles with zone of inhibition 19 mm and 18 mm respectively. The Fig. 6. (a) SEM image of the as-synthesized Mn3O4 nanoparticles and (b) energy dispersive X-ray spectroscopy of Mn3O4 nanoparticles. Table 2 Zone of Inhibition results of the susceptibility of different microbial strains tested against standard antibiotics. Zone of Inhibition (mm) Mn_2O_3 NPs AntibioticGentamycin (30 mg/ml) Antibioticfluconazole (50 mg/ml) E. coli 10 mm 22 mm – S. aureus 19 mm 21 mm – P. aeruginosa 12 mm 22 mm – B. subtilis 18 mm 22 mm – C. albicans 18 mm – 20 mm A. flavus 14 mm – 20 mm.

References:

[1] C. Burda, X. B. Chen, R. Narayanan, and M. A. El-Sayed, “Chemistry and properties of nanocrystals of different shapes,” Chemical Reviews, vol. 105, no. 4, pp. 1025–1102, 2005.

[2] D. Yan, S. Cheng, R. F. Zhuo et al., “Nanoparticles and 3D sponge-like porous networks of manganese oxides and their microwave absorption properties,” Nanotechnology, vol. 20, no. 10, Article ID 105706, 2009.

[3] Y. W. Tan, L. R. Meng, Q. Peng, and Y. D. Li, “One-dimensional single-crystalline Mn3O4 nanostructures with tunable length and magnetic properties of Mn3O4 nanowires,” Chemical Communications, vol. 47, no. 4, pp. 1172–1174, 2011.

[4] X. Zhang, Z. Xing, Y. Yu et al., “Synthesis of Mn3O4 nanowires and their transformation to LiMn2O4 polyhedrons, application of LiMn2O4 as a cathode in a lithium-ion battery,” CrystEngComm, vol. 14, no. 4, pp. 1485–1489, 2012.

[5] R. Ma, Y. Bando, L. Zhang, and T. Sasaki, “Layered MnO2 nanobelts: hydrothermal synthesis and electrochemical measurement,”Advanced Materials, vol. 16, no. 11, pp. 918–922, 2004.

[6] F. Y. Cheng, J. Z. Zhao, W. Song et al., “Facile controlled synthesis of MnO2 nanostructures of novel shapes and their application in batteries,” Inorganic Chemistry, vol. 45, no. 5, pp. 2038–2044, 2006

[7] G. L. Xu, Y. F. Xu, H. Sun et al., “Facile synthesis of porous MnO/C nanotubes as a high capacity anode material for lithium ion batteries ,” Chemical Communications, vol. 48, pp. 8502– 8504, 2012.

[8] Adschiri, T.; Hakuta, Y.; Arai, K. Hydrothermal synthesis of metal oxide fine particles at supercritical conditions. *Ind. Eng. Chem. Res.* **2000**, *39*, 4901–4907

[9] Hakuta, Y.; Hayashi, H.; Arai, K. Hydrothermal synthesis of photocatalyst potassium hexatitanate nanowires under supercritical water conditions. *J. Mater. Sci.* **2004**, *39*, 4977–4980

[10] Hakuta, Y.; Ura, H.; Hayashi, H.; Arai, K. Effects of hydrothermal synthetic conditions on the particle size of γ-□AlO(OH) in sub and supercritical water using a flow reaction system. *Mater. Chem. Phys.* **2005**, *93*, 466–472.

[11] Lee, J.H.; Ham, J.Y. Synthesis of manganese oxide particles in supercritical water. *Korean J. Chem. Eng.* **2006**, *23*, 714–719.

[12] G.A.M. Ali, O.A. Fouad, S.A. Makhlouf, M.M. Yusoff, K.F. Chong, Co3O4/SiO2 nanocomposites for supercapacitor application, J. Solid State Electrochem. 18 (2014) 2505–2512

[13] Y. Dai, K. Wang, J.Y. Xie, From spinel Mn3O4 to layered nanoarchitectures using electrochemical cycling and the distinctive pseudocapacitive behavior, Appl. Phys. Lett. 90 (2007).

[14] S. Devaraj, N. Munichandraiah, Effect of crystallographic structure of MnO2 on its electrochemical capacitance properties, J. Phys. Chem. C. 112 (2008) 4406–4417.

[15] D.P. Dubal, W.B. Kim, C.D. Lokhande, Surfactant assisted electrodeposition of MnO2 thin films: improved supercapacitive properties, J. Alloy. Compd. 509 (2011) 10050–10054.

[16] M.M. Yao, Z.H. Hu, Y.F. Liu, P.P. Liu, Z.H. Ai, O. Rudolf, 3D hierarchical mesoporous roselike NiO nanosheets for high-performance supercapacitor electrodes, J. Alloy. Compd. 648 (2015) 414–418.

[17] M.M. Momeni, Z. Nazari, A. Kazempour, M. Hakimiyan, S.M. Mirhoseini, Preparation of CuO nanostructures coating on copper as supercapacitor materials, Surf. Eng. 30 (2014) 775–778.

[18] G.A.M. Ali, O.A. Fouad, S.A. Makhlouf, M.M. Yusoff, K.F. Chong, Optical and electrochemical properties of Co3O4/SiO2 nanocomposite, Adv. Mater. Res. 1133 (2016) 447–451.

[19] G.A.M. Ali, O.A.G. Wahba, A.M. Hassan, O.A. Fouad, K.F. Chong, Calcium-based nanosized mixed metal oxides for supercapacitor application, Ceram. Int. 41 (2015) 8230–8234.

[20] D.P. Dubal, C.D. Lokhande, Significant improvement in the electrochemical performances of nano-nest like amorphous MnO2 electrodes due to Fe doping, Ceram. Int. 39 (2013) 415–423.

[21] R.B. Rakhi, D.K. Cha, W. Chen, H.N. Alshareef, Electrochemical energy storageocoils and metal oxides nano particles

[22] Zhang, X.-Y.; Han, L.-Q.; Sun, S.; Wang, C.-Y.; Chen, M.-M. MnO2/C composite electrodes free of conductive enhancer for supercapacitors. J. Alloys Compd. 2015, 653, 539–545.

[23] Zhang, Q.-H.; Li, S.-P.; Sun, S.-Y.; Yin, X.-S.; Yu, J.-G. Lithium selective adsorption on 1-D MnO2 nanostructure ion-sieve. Adv. Powder Technol. 2009, 20, 432–437.

[24] Della-Puppa, L.; Komarek, M.; Bordas, F.; Bollinger, J.-C.; Joussein, E. Adsorption of copper, cadmium, lead and zinc onto a synthetic manganese oxide. J. Colloid Interface Sci. 2013, 399, 99–106. [CrossRef] [PubMed]

[25] Julien, C.; Massot, M.; Poinsignon, C. Lattice vibrations of manganese oxides. Part I. Periodic structures. Spectrochim. Acta A 2004, 60,

[26] 689–700. [CrossRef] 19. Clearfield, A. Role of ion exchange in solid-state chemistry. Chem. Rev. 1988, 88, 125–148.

[27] Biswal, A.; Tripathy, B.C.; Sanjay, K.; Meyrick, D.; Subbaiah, T.; Minakshi, M. Influence of the microstructure and its stability on the electrochemical properties of EMD produced from a range of precursors. J. Solid State Electrochem. 2013, 17, 3191–3198.

[28] Biswal, A.; Tripathy, B.C.; Sanjay, K.; Subbaiah, T.; Minakshi, M. Electrolytic manganese dioxide (EMD): A perspective on worldwide production, reserves and its role in electrochemistry. RSC Adv. 2015, 5, 58255–58283.

[29] Huang, M.; Li, F.; Dong, F.; Zhang, Y.X.; Zhang, L.L. MnO2 -based nanostructures for high performance supercapacitors. J. Mater. Chem. A 2015, 3, 21380–23423.

[30] Julien, C.M.; Mauger, A.; Zaghib, K. Surface effects on electrochemical properties of nano-sized LiFePO4 . J. Mater. Chem. 2011, 21, 9955–9968.

[31] Vondrak, J.; Jakubec, I.; Bludska, J. Electrochemical insertion of lithium in manganese oxide. J. Power Sources 1985, 14, 141–147.

[32] Zhang, Y.; Mo, Y. Preparation of MnO2 electrodes coated by Sb-doped SnO2 and their effect on electrochemical performance for supercapacitor. Electrochim. Acta 2014, 142, 76–83.

[33] Feng, L.; Zhang, Y.; Wang, R.; Zhang, Y.; Bai, W.; Ji, S.; Xuan, Z.; Yang, J.; Zheng, Z.; Guan, H. Preparation of PPy-coated MnO2 hybrid micromaterials and their improved cyclic performance as anode for lithium-ion batteries. Nanoscale Res. Lett. 2017, 12, 518.

[34] Devaraj, S.; Munichandraiah, N. High capacitance of electrodeposited MnO2 by the effect of a surface-active agent. Electrochem. Solid-State Lett. 2005, 8, A373–A377.

[35] Chou, S.-L.; Wang, J.-Z.; Chew, S.-Y.; Liu, H.-K.; Dou, S.-X. Electrodeposition of MnO2 nanowires on carbon nanotube paper as free-standing, flexible electrode for supercapacitors. Electrochem. Commun. 2008, 10, 1724–1727.

[36] Livage, J.; Sanchez, C.; Henry, M.; Doeuff, S. The chemistry of the sol-gel process. Solid State Ion. 1989, 32–33, 633–638.

[37] Yu, P.; Zhang, X.; Wang, D.; Wang, L.; Ma, Y. Shape controlled synthesis of 3D hierarchical MnO2 nanostructures for electrochemical supercapacitors. Cryst. Growth Des. 2009, 9, 528–533.

[38] Liu, X.; Chen, C.; Zhao, Y.; Jia, B. A review on the synthesis of manganese oxide nanomaterials and their applications on lithium-ion batteries. J. Nanomater. 2013, 2013, 736375.

[39] Wang, X.; Li, Y. Selected-control hydrothermal synthesis of α- and β-MnO2 single crystal nanowires. J. Am. Chem. Soc. 2002, 124, 2880–2881.

[40] Wei, M.; Konishi, Y.; Zhou, H.; Sugihara, H.; Arakawa, H. Synthesis of single-crystal manganese dioxide nanowires by a soft chemical process. Nanotechnology 2005, 16, 245–249.

[41] Yuan, Z.Y.; Ren, T.Z.; Du, G.H.; Su, B.L. Facile preparation of single-crystalline nanowires of γ-MnOOH and β-MnO2 . Appl. Phys. A 2005, 80, 743–747. [CrossRef] 35. Sugantha, M.; Ramakrishnan, P.A.; Hermann, A.M.; Ginley, D.S. Nanostructured MnO2 for Li batteries. Int. J. Hydrogen Energy 2003, 28, 597–600.

[42] Kumari Latha, Li W.Z., Vannoy Charles H., Leblanc Roger M., Wang D.Z. Synthesis, characterization and optical properties of $Mg(OH)_2$ micro-/nano-structure and its conversion to MgO. *Ceramics International.* 2009;**35**:3355–3364.

[43] Selvamani T., Yagyu T., Kawasaki S., Mukhopadhyay I. Easy and effective synthesis of micrometer-sized rectangular MgO sheets with very high catalytic activity. *Catalysis Communications.* 2010;**11**:537–541.

[44] Deneen Nowak Julia, Barry Carter C. Forming contacts and grain boundaries between MgO nanoparticles. *Journal of Material Science.* 2009;**44**:2408–2418.

[45] Ilyina E.V., Mishakov I.V., Vedyagin A.A. Preparation of nanocrystalline VMg(OH)x and VOx· MgO from organometallic precursors. *Inorganic Materials.* 2009;**45**(11):1267–1270.

[46] Venkateswara Rao K., Sunandana C.S. Structure and microstructure of combustion synthesized MgO nanoparticles and nanocrystalline MgO thin films synthesized by solution growth route. *Journal of Material Science.* 2008;**43**:146–154.

[47] Comini Elisabetta, Faglia Guido, Ferroni Matteo, Ponzoni Andrea, Vomiero Alberto, Sberveglieri Giorgio. Metal oxide nanowires: preparation and application in gas sensing. *Journal of Molecular Catalysis A: Chemical.* 2009;**305**:170–177.

[48] Rezaei Mehran, Khajenoori Majid, Nematollahi Behzad. Synthesis of high surface area nanocrystalline MgO by pluronic P123 triblock copolymer surfactant. *Powder Technology.* 2011;**205**:112–116.

[49] Fedorov P.P., Tkachenko E.A., Kuznetsov S.V., Voronov V.V., Lavrishchev S.V. Preparation of MgO nanoparticles. *Inorganic Materials.* 2007;**43**(5):502–504.

[50] Sasaki Takeshi, Shimizu Yoshiki, Koshizaki Naoto. Preparation of metal oxide-based nanomaterials using nanosecond pulsed laser ablation in liquids. *Journal of Photochemistry and Photobiology A: Chemistry.* 2006;**182**:335–341.

[51] Makhluf Shirly., Dror Rachel., Nitzan Yeshayahu., Abramovich Yaniv., Jelinek Raz., Gedanken Aharon. Microwave assisted synthesis of nanocrystalline MgO and its use as a bacteriocide. *Advanced Functional Materials.* 2005;**15**:1708–1715.

[52] Esmaeili Elaheh, Khodadadi Abasali, Mortazavi Yadollah. Microwave-induced combustion process variables for MgO nanoparticle synthesis using polyethylene. *Journal of the European Ceramic Society.* 2009;**29**:1061–1068.

[53] Phuoc Tran X., Howard Bret H., Martello Donald V., Soong Yee, Chyu Minking K. Synthesis of Mg(OH)2, MgO, and Mg nanoparticles using laser ablation of magnesium in water and solvents. *Optics and Lasers in Engineering.* 2008;**46**:829–834.

[54] Djerdj Igor, Arcon Denis, Jaglicic Zvonko, Niederberger Markus. Nonaqueous synthesis of metal oxide nanoparticles: Short review and doped titanium dioxide as case study for the preparation of transition metal-doped oxide nanoparticles. *Journal of Solid State Chemistry.* 2008;**181**:1571–1581.

[55] Zhang Lingling, Jiang Yunhong, Ding Yulong, Povey Malcolm, York David. Investigation into the antibacterial behaviour of suspensions of ZnO nanoparticles (ZnO nanofluids) *Journal of Nanoparticle Research.* 2007;**9**(3):479–489.

[56] Zhu Kake, Hu Juncheng, Kuebel Christian, Richards Ryan. Efficient preparation and catalytic activity of MgO (111) nanosheets. *Angewandte Chemie.* 2006;**118**:43.

[57] Venkateswara Rao K., Sunandana C.S. Structure and microstructure of combustion synthesized MgO nanoparticles and nanocrystalline MgO thin films synthesized by solution growth route. *Journal of Materials Science.* 2008;**43**:146–154.

[58] Lei Huang, Dianqing Li, Yanjun Lin, Evans David G., Xue Duan. Influence of nano-MgO particle size on bactericidal action against Bacillus subtilis var. niger. *Chinese Science Bulletin.* 2005;**50**(6):514–519.

[59] Huang Lei, Li Dian-Qing, Lin Yan-Jun, Wei Min, Evans David G., Duan Xue. Controllable preparation of Nano-MgO and investigation of its bactericidal properties. *Journal of Inorganic Biochemistry.* 2005;**99**:986–993.

[60] Gordon Tamar, Perlstein Benny, Houbara Ofir, Felner Israel, Banin Ehud, Margel Shlomo. Synthesis and characterization of zinc/iron oxide composite nanoparticles and their antibacterial properties. *Colloids and Surfaces A: Physicochemical and Engineering Aspects.* 2011;**374**:1–8.